J. Univ. Kuwait (Sci.) **20**, 1993

The role of magnetizing reactance in steady-state performance of induction generators

MOHAMED H. SALAMA

Department of Electrical and Computer Engineering, University of Kuwait, P.O. Box 5969, Safat 13060, Kuwait

ABSTRACT

The paper presents a computational method for predicting the load performance of a stand-alone induction generator. A mathematical model derived from the generator equivalent circuit is used as the basis for the computation.

In the model, the minimum value of capacitance necessary for the machine to self-excite is the critical factor. This minimum value is both load- and speed-dependent.

The magnetizing reactance is nonlinear, and its value is affected by the capacitance used for excitation. This nonlinear variation of magnetizing reactance related to the exciting capacitance defines a critical maximum and a critical minimum value of reactance.

The terminal voltage, terminal frequency and generator efficiency are calculated from the model for a wide range of load impedances and power factors. Close correlation between measured and calculated results gives confidence in the model, which provides a basis for VAR compensator design in stand-alone micro-hydro systems.

LIST OF SYMBOLS

a = Per unit frequency (output frequency/rated frequency)
b = Per unit speed (rotor speed/synchronous speed)
R_1, R_2 = Stator and rotor resistance per phase referred to stator, ohm
X_1, X_2 = Stator and rotor reactance per phase referred to stator, ohm
X_m = Magnetizing reactance per phase, ohm
E_g = Air-gap voltage, V
$X_{s\,max}$ = Maximum unsaturated magnetizing reactance, ohm
C = Terminal self-excitation capacitance per phase, F
C_{min} = Minimum value of capacitance required for self-excitation, F
C_{max} = Maximum value of capacitance required for self-excitation, F
X_c = Self-excitation capacitive reactance per phase, ohm
R = Load resistance per phase, ohm
X = Load reactance per phase at rated frequency, ohm
V_{out} = Terminal voltage across the load per phase, V
n_g = Generator efficiency

INTRODUCTION

The steady-state performance of isolated induction generators has attracted the attention of several investigators during the past decade. In particular, Melkebeek & Novotny (1983a, b) have investigated both the steady-state modeling of regeneration and self-excitation of induction motors as well as the influence of saturation on motor dynamics. Ouazene & Macpherson (1983) described a variable-speed drive using capacitor-excited squirrel cage induction machines. They presented a reasonable model for the performance evaluation based on the steady-state equivalent circuit. Murthy & Tandon (1985) also developed a model based on the usual equivalent circuit of the induction motor, and by modifying the value of the unsaturated magnetizing reactance, obtained complex roots giving rise to oscillatory behaviour as well as the load voltage, frequency and current. Later, Yegna Narayanan & Johnny (1986) developed a digital computer method for predicting the steady-state performance of a self-excited induction generator for a given speed.

Grantham *et al.* (1989) calculated the output voltage and frequency of a stand-alone induction generator under resistive loading conditions and a no-load condition. On comparing theoretical and experimental results, excellent agreement was obtained when the rotor parameters were considered to have their values for low slip frequencies. Later, their theory was extended to include the transient build-up voltage during the initiation stage of self-excitation. Recently, Malik & Al-Bahrani (1990) examined the influence of the excitation capacitor on the steady-state performance characteristics of an isolated self-excited induction generator feeding a balanced load. They stated that the terminal voltage is independent of the load power factor and is only affected by the magnitude of the load impedance. This paper is concerned with the steady-state performance of an isolated self-excited induction generator when feeding different types of load and taking into consideration the non-linear behavior of the magnetizing reactance. To achieve this, a mathematical model based on the equivalent circuit of the machine is used to enable the role of the magnetizing reactance to be investigated. This is carried out while accounting for magnetic saturation in the D-Q model of the generator by using appropriate values of stator and rotor inductance both of which include the magnetizing reactance. In another paper by the author (Salama 1993), a mathematical model, based on the stationary reference frame, is used to compute the range of capacitance necessary to ensure the initiation and the transient build-up process of the air-gap voltage. However, the steady-state analysis of the self-excited induction generator is rather complex because:

(1) Both the terminal voltage and frequency are unknown parameters.
(2) The magnetizing reactance of the machine has a non-linear characteristic.

Therefore, this paper presents a systematic procedure for computing the steady-state performance of a stand-alone self-excited generator.

A MATHEMATICAL MODEL

The analysis pursued hereafter is based on the assumption that both the initiation and the transient build-up process of the air-gap voltage has been successfully achieved by one way or another. Thus it is assumed that the air-gap voltage of the

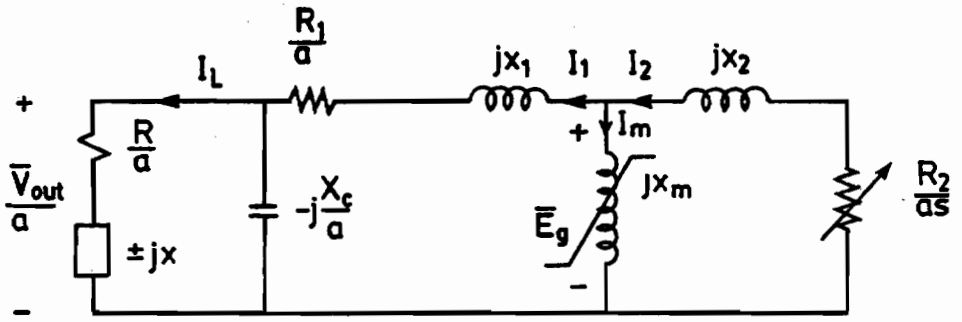

Fig. 1. The steady-state equivalent circuit of an induction generator.

generator has reached its steady-state value E_g. The steady-state equivalent circuit of an isolated self-excited induction generator which feeds a balanced 3-phase load is shown in Fig. 1. This equivalent circuit is further simplified (Fig. 2). where the R_L and X_L parameters injected into the equivalent circuit depend on the type of load connected at the terminals of the generator and the capacitor required for the self-excitation process. These parameters are presented in Appendix 1. Application of the node-voltage analysis for the circuit shown in Fig. 2 yields

$$E_g Y_1 + E_g Y_2 + E_g Y_3 = 0 \tag{1}$$

Since $E_g \neq 0$, thus

$$Y_1 + Y_2 + Y_3 = 0 \tag{2}$$

Equating the real and reactive parts of Eqn (2) to zero, the following expressions are obtained:

$$\frac{R_L + (R_1/a)}{[R_L + (R_1/a)]^2 + (X_1 - X_L)^2} + \frac{[R_2/(a-b)]}{[R_2/(a-b)]^2 + X_2^2} = 0 \tag{3}$$

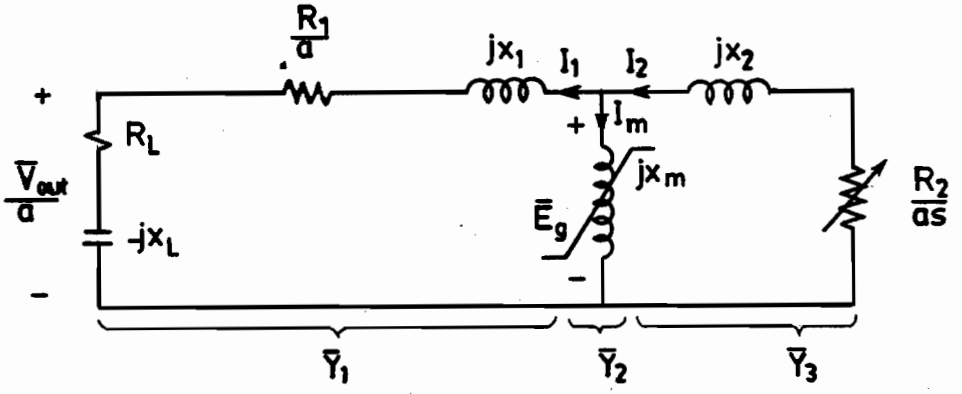

Fig. 2. A simplified equivalent circuit of induction generator.

and

$$-\frac{1}{X_m}-\frac{X_2}{[R_2/(a-b)]^2+X_2^2}-\frac{X_1-X_L}{(R_L+R_1/a)^2+(X_1-X_L)^2}=0 \tag{4}$$

Eqn (3) will be used to determine the terminal frequency f_s, while Eqn (4) will be used to obtain the effective magnetizing reactance.

MACHINE DATA

The machine used in the investigation is a 380 V, 50 Hz, 1 kW, 4 pole, 30 squirrel-cage induction machine. In order to estimate the machine parameters, several tests were carried out. However, for the rotor parameters, recommendations suggested by Grantham (1985) for accurate values of rotor impedance were implemented. A locked-rotor variable-frequency test was also conducted. The values of rotor parameters corresponding to a slip of 5 Hz were used for the analysis; the machine parameters were

$$R_1 = 8{\cdot}5 \text{ ohm/phase} \qquad X_1 = 15{\cdot}715 \text{ ohm/phase}$$

$$R_2 = 3{\cdot}589 \text{ ohm/phase} \qquad X_2 = 18{\cdot}060 \text{ ohm/phase}$$

$$X_{s\,\max} = 133{\cdot}7 \text{ ohm/phase}$$

DETERMINATION OF THE OUTPUT FREQUENCY

For a specified load impedance and a given capacitance for self-excitation at a particular rotor speed, Eqn (3) is rewritten as a polynomial in terms of the per-unit frequency ($a = f_s/f_{\text{rated}}$), thus

$$P_7 a^7 + P_6 a^6 + P_5 a^5 + P_4 a^4 + P_3 a^3 + P_2 a^2 + P_1 a + P_0 = 0 \tag{5}$$

The coefficients of the polynomial (P_0 to P_7) in Eqn (5) for the four types of loading suggested in the analysis are presented in Appendix 2.

THE EFFECTIVE VALUE OF THE MAGNETIZING REACTANCE

By manipulating Eqn (4), the magnetizing reactance can be derived as

$$X_m = \frac{[R_L + (R_1/a)][X_2^2 + (R_2/a - b)^2]}{(X_1 - X_L)[R_2/(a-b)] - X_2[R_L + (R_1/a)]} \tag{6}$$

Having determined the value of a from Eqn (5), according to the type of load at the terminals of the generator, Eqn (6) can then be used to determine the effective value of X_m.

The X_m-curves shown in Figs 3, 4 and 5 describe the non-linear characteristics of the magnetizing reactance as the self-excitation capacitance is varied. Since the $X_{s\,\max}$ line represents the maximum unsaturated magnetizing reactance of the machine, the operating range of the machine as an induction generator will be determined by the part of the curve located under the $X_{s\,\max}$ line.

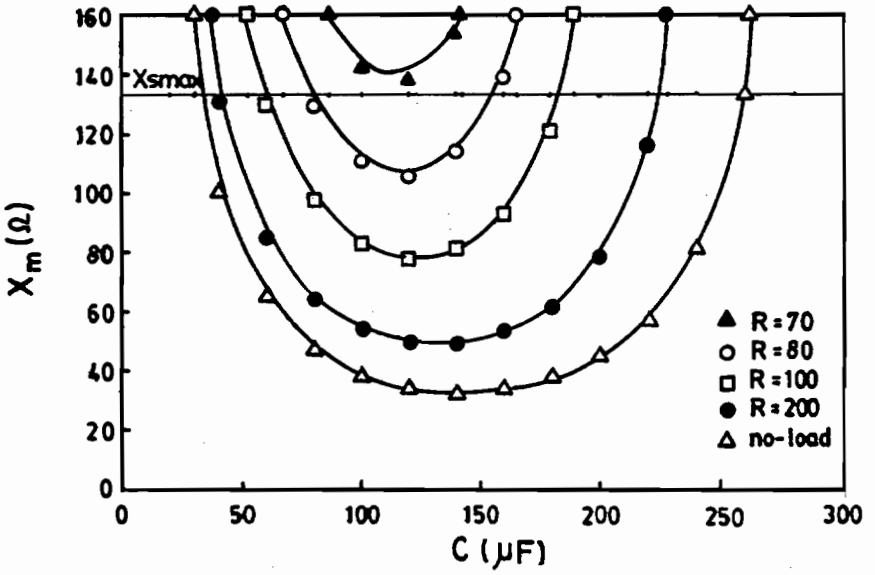

Fig. 3. Variation of X_m with C and R.

The curves in Fig. 3 indicate that as the resistive load is decreased the range of capacitance which ensures the initiation of the self-excitation process will be reduced, although the minimum value of the magnetizing reactance will be increased. The minimum value of the magnetizing reactance will reach $X_{s\,max}$ when the resistive load reaches $R_{critical}$ at which C_{min} will be equal to C_{max}. This is true

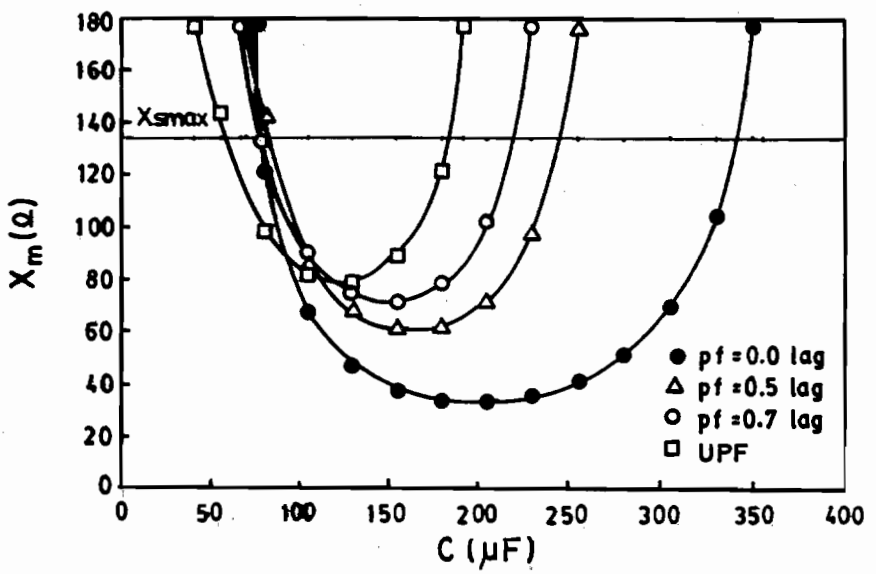

Fig. 4. Variation of X_m with C and lagging load power factors at $|Z| = 100\ \Omega$ and rotor speed 1250 rpm.

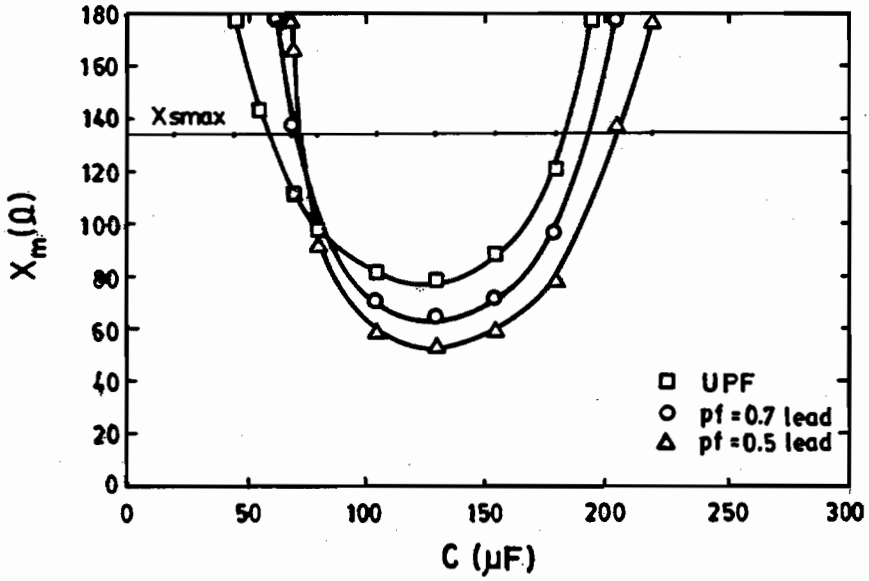

Fig. 5. Variation of X_m with C and leading power factors at $|Z| = 100\ \Omega$ and rotor speed 1250 rpm.

since the intersection of the $X_{s\,max}$ line with a characteristic curve determines the limits of the capacitance range (C_{min} and C_{max}) necessary to initiate the self-excitation process in the air-gap of the machine.

Figs 4 and 5 reveal that the effective value of the magnetizing reactance is highly influenced by loads with variable lagging power factors. However, minor changes are also observed for leading power factor loads.

THE AIR-GAP VOLTAGE

In order to obtain the steady-state performance of the generator, the steady-state value of the air-gap voltage is needed. The mathematical technique adopted to compute the air-gap voltage E_g starts by calculating the value of X_m which corresponds to the thermal impedance, the driving speed and the capacitance used for the self-excitation process. The magnetization curve of the machine obtained from the no-load test is then used to obtain a curve representing $E_g - X_m$.

The $E_g - X_m$ curve shown in Fig. 6 is expressed by an nth order polynominal. It is found that for $n = 5$, the accuracy obtained in comparison to the experimental curve was about 98%. The effective value of X_m is then used to find the operating value of E_g at rated frequency.

THE GENERATED TERMINAL VOLTAGE

The equivalent circuit (Fig. 2) will be used in the mathematical procedure to compute the terminal voltage. The expression for V_{out} will depend on the type of

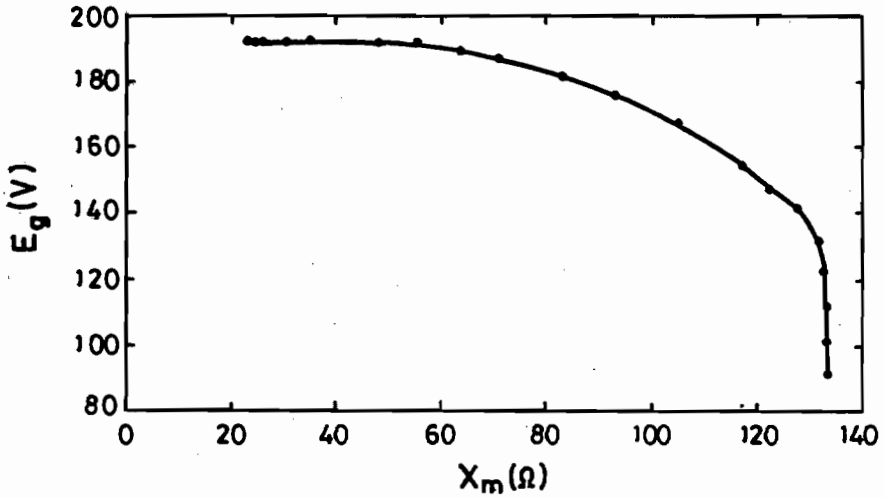

Fig. 6. Variation of E_g with X_m.

load connected to the terminals of the generator. For an inductive load ($Z = R + jX$), the amplitude of the terminal voltage will be

$$V_{out} = aE_g \frac{a^2(XX_c)^2 + (RX_c)^2}{a^6(XX_1)^2 + a^4(R^2X_1^2 + R_1^2X_1^2 - 2X_1X^2X_c - 2X_1^2XX_c) + a^2(X^2X_c^2 + R^2R_1^2 + 2XX_1X_c^2 + X_1^2X_c^2 - 2X_1X_c^2R + 2XX_cR_1^2) + (R^2X_c^2 + 2RR_1X_c^2 + R_1^2X_c^2)} \quad (7)$$

The terminal voltage for a resistive load can be obtained from Eqn (7) by substituting $X = 0$. For the no-load case, the terminal voltage can be obtained by multiplying the expression for V_{out} for a resistive load and taking the limit as $R \to \infty$. For a capacitive load, the amplitude of the terminal voltage will be

$$V_{out} = aE_g \frac{a^2(XX_c)^2 + (RX_c)^2}{a^6(X_1X)^2 + a^4(R^2X_1^2 + R_1^2X^2 + 2X_1^2XX_c - 2X_1X^2X_c) + a^2(X_1^2X^2 - 2XX_1X_c^2 + R^2R_1^2 + X^2X_c^2 - 2R^2X_1X_c + 2R^2X_1X_c) + (R^2X_c^2 + 2RR_1X_c^2 + R_1^2X_c^2)} \quad (8)$$

THE GENERATOR TERMINAL CURRENT

The terminal current is expressed as

$$I = \frac{(V_{out}/a)}{(R/a)^2 + X^2} \quad (9)$$

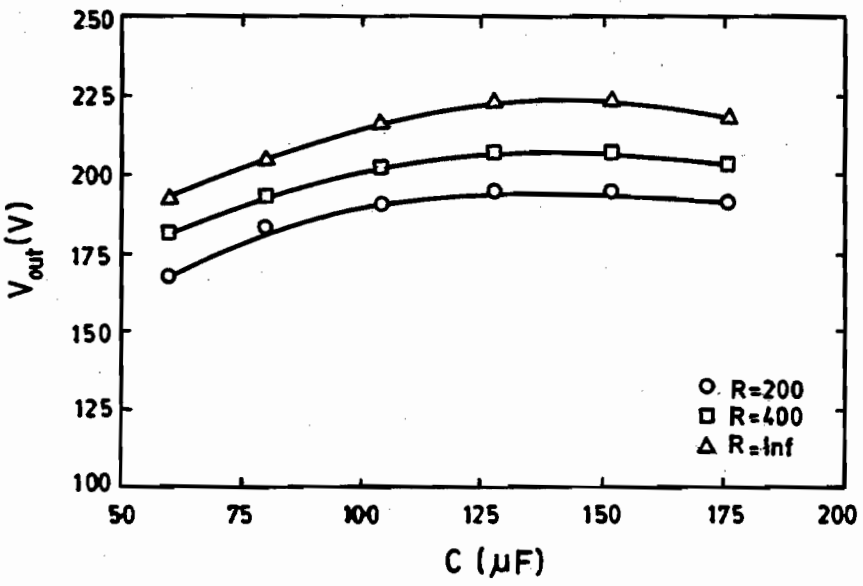

Fig. 7. Variation of output voltage with C and R at rotor speed 1250 rpm.

GENERATOR EFFICIENCY

By neglecting both the rotor and stator core losses, the power flow diagram for the generator will be simplified such that:

$$\text{The output electrical power } P_{out} = 3V_{out} \cdot I \cdot \frac{(R/a)}{(R/a)^2 + X^2} \tag{10}$$

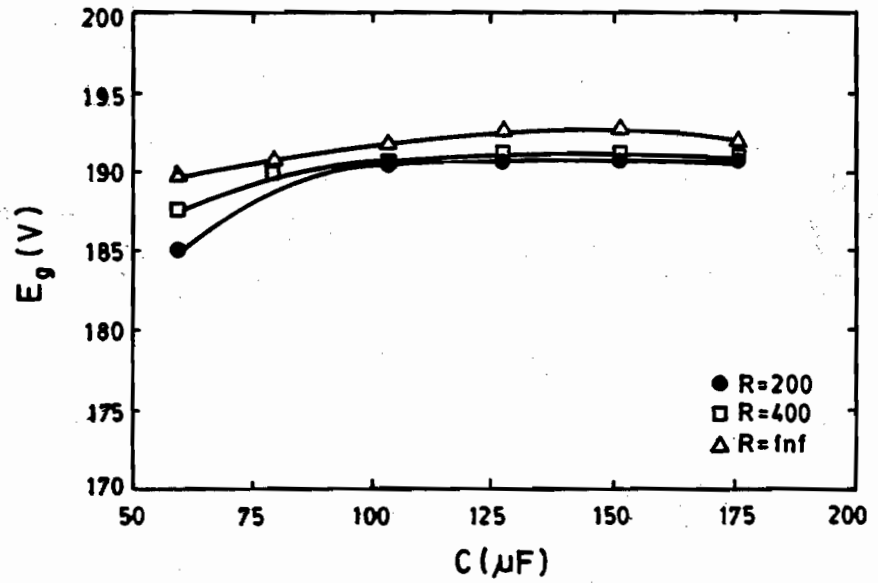

Fig. 8. Variation of air-gap voltage with C and R at rotor speed 1250 rpm.

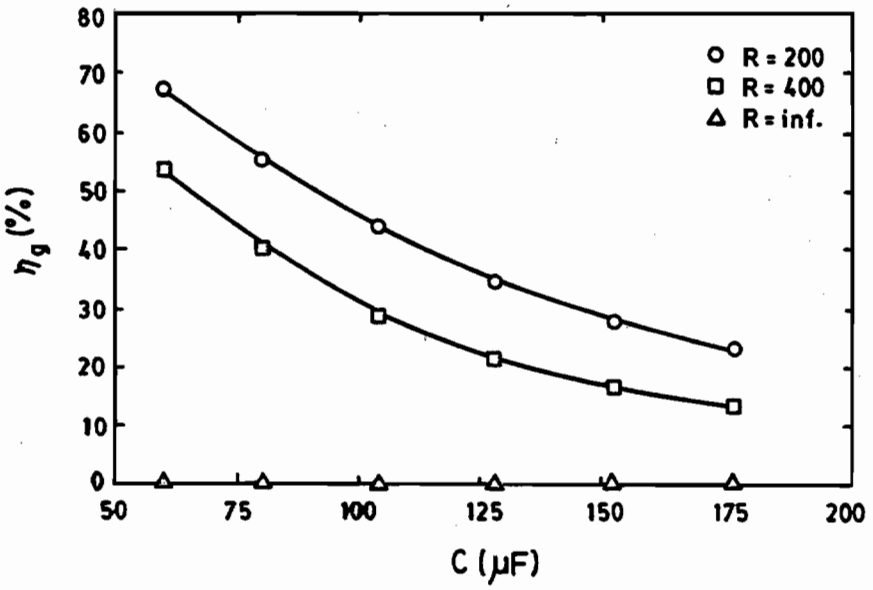

Fig. 9. Variation of efficiency with C and R at rotor speed 1250 rpm.

And the mechanical power input to the rotor of the generator is given as

$$P_{\text{mech}} = -3I_{\text{rotor}}^2 R_2\left(\frac{b}{a-b}\right) \tag{11}$$

The generator efficiency $ng = \dfrac{P_{\text{out}}}{P_{\text{mech}}} \times 100.$

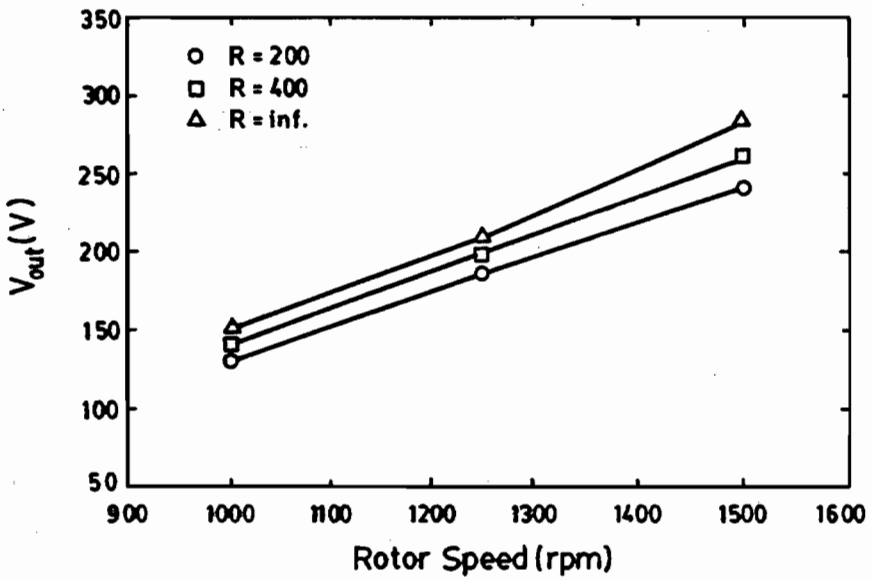

Fig. 10. Variation of output voltage with rotor speed and R at $C = 90$ μF.

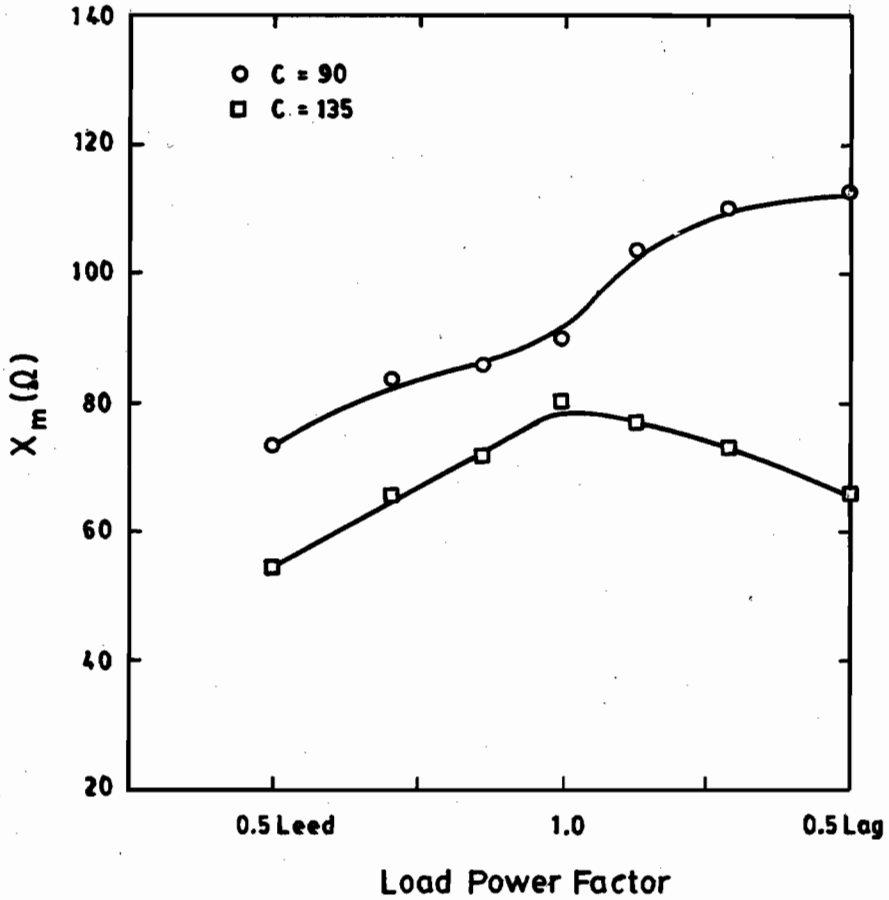

Fig. 11. Variation of magnetizing reactance with load power factor and C at rotor speed 1250 rpm.

THE STEADY-STATE PERFORMANCE

The proposed mathematical model was tested against the experimental results which were carried out with two different balanced 3-phase load resistances of values higher than the critical value $R_{critical}$ (discussed by Salama 1993), and with $C = 90\ \mu F$, which is higher than C_{min}. The results obtained are presented in Table 1.

DISCUSSION OF RESULTS

Part of the computed results obtained show and support similar cases obtained by other investigators (Tandon *et al.* 1984; Grantham *et al.* (1989); Malik & Al-Bahrani 1990).

The mathematical model was tested for a speed below the corresponding synchronous speed of the machine. The selection of such a speed was motivated by the desire to demonstrate that the self-excited generator will perform whether the driving speed is below or above synchronous speed. Of course, better performance is expected when the machine is driven at speeds higher than synchronous speed.

Table 1. Comparison between theoretical and experimental results

Speed rpm	1000				1250				1500			
R ohm	100		200		100		200		100		200	
Result	Exp.	Theo.	Exp.	Theo.	Exp.	Theo.	Exp.	Theo.	Exp.	Theo.	Exp.	Theo.
V_{out} V	90·0	92·6	128·0	130·4	155·0	158·5	185·0	187·0	197·0	198·8	240·0	242·3
f_s Hz	31·5	31·6	32·0	32·1	38·0	38·8	39·0	39·5	45·0	45·2	46·0	46·2
i_1 A	2·00	1·89	2·50	2·46	3·90	3·82	4·40	4·28	5·60	5·45	6·40	6·44
P_{out} W	243	257	245	255	720	754	513	525	1166	1186	886	881

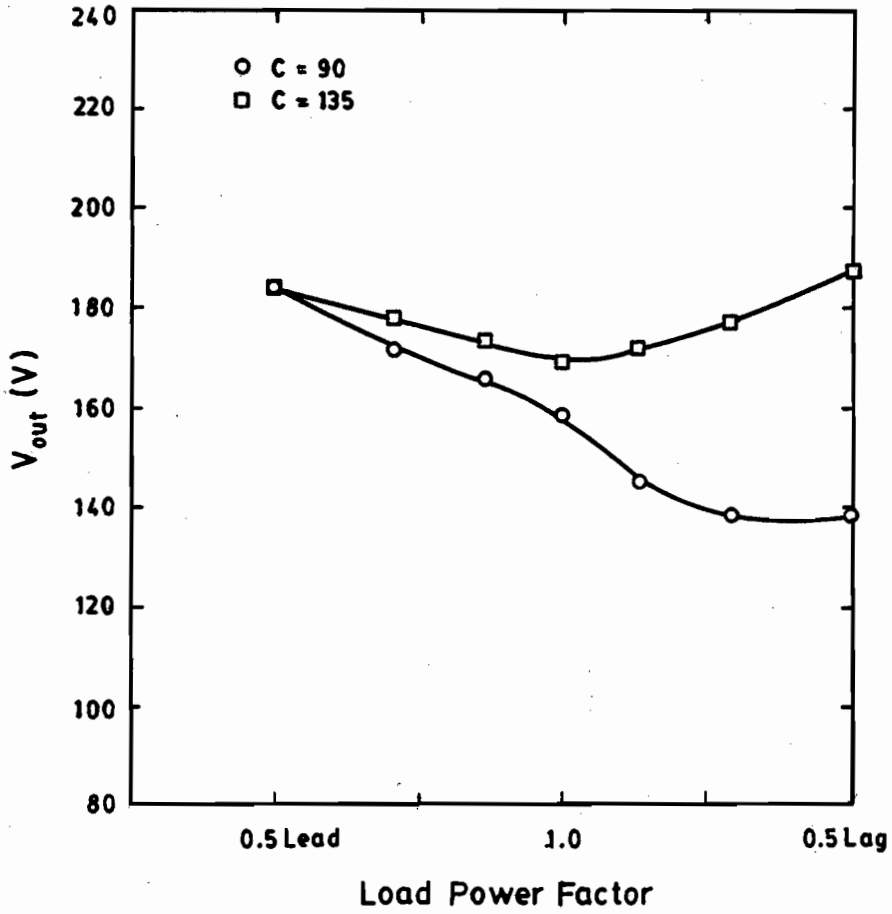

Fig. 12. Variation of output voltage with load power factor and C at rotor speed 1250.

The steady-state performance characteristics presented in Figs 7 to 10 reveal the following features:

(i) Highest values of the terminal voltage are obtained at no-load conditions (Fig. 7). This is a fact for all types of generator, DC or AC.
(ii) The air-gap voltage will reach an almost constant value if the capacitance connected at the terminals of the generator is of a value $\gg C_{min}$ (Fig. 8).
(iii) Higher efficiency is obtained with capacitance values close to C_{min} (Fig. 9).
(iv) The output terminal voltage builds up almost linearly with rotor speed (Fig. 10). Hence it is expected that the generator will develop still higher terminal voltages at speeds above synchronous.

EFFECT OF LOAD POWER FACTOR

The load power factor has a considerable influence on the effective value of the magnetizing reactance (Fig. 11). For a terminal capacitance close to C_{min}, the

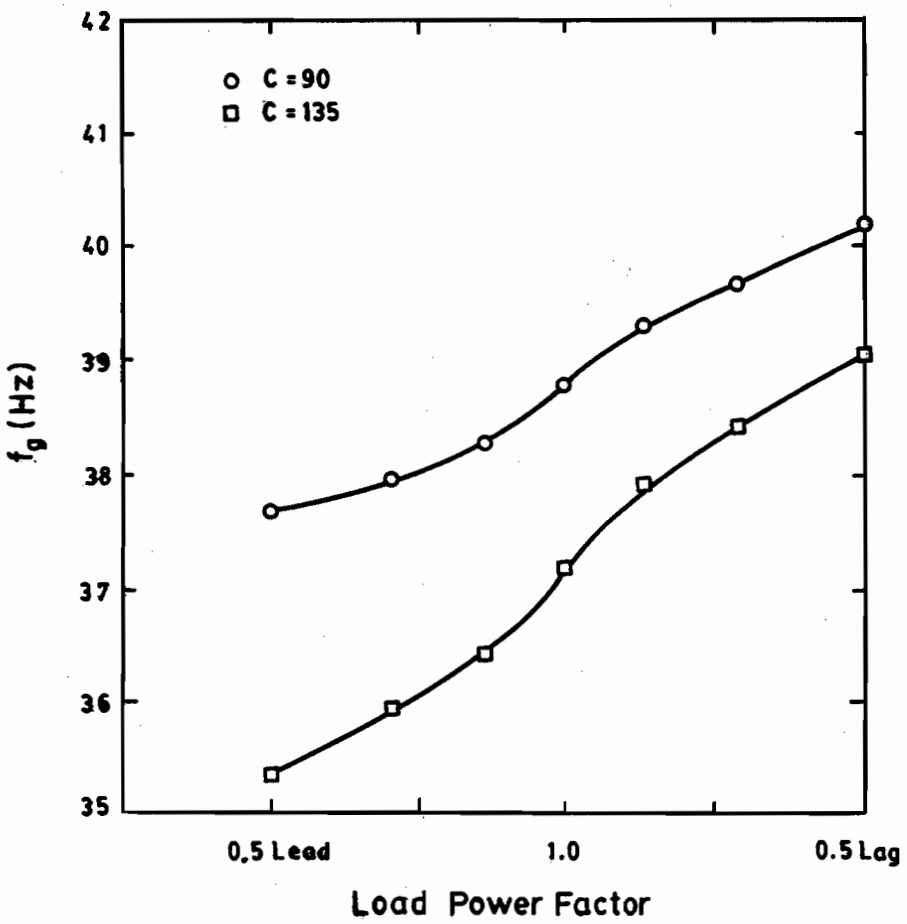

Fig. 13. Variation of excitation frequency with load power factor and C at rotor speed 1250 rpm.

change of X_m about its value corresponding to unity power factor is almost equal. However, for a terminal capacitance higher than C_{min}, the results indicate that the highest value of X_m is obtained at a power factor of unity.

The nonlinearity of the magnetizing reactance is demonstrated by the results obtained for the terminal voltage V_{out} (Fig. 12). Minimum terminal voltage is obtained at unity power factor, when the terminal capacitance is far from C_{min}. However, the characteristic curve is almost symmetrical about unity power factor for values of capacitance close to C_{min}. The terminal frequency f_s is also influenced by the nonlinearity of the magnetizing reactance (Fig. 13). By taking the value of f_s at unity power factor as a base, positive changes in f_s are recorded for lagging power factors, while negative changes of almost the same magnitude are obtained for leading power factors. The nonlinear behaviour of the magnetizing reactance is again demonstrated in the computed results obtained for the efficiency of the generator *ng* (Fig. 14). By taking the efficiency at unity power factor as a reference, the rise in efficiency obtained for lagging power factor is almost of the same magnitude

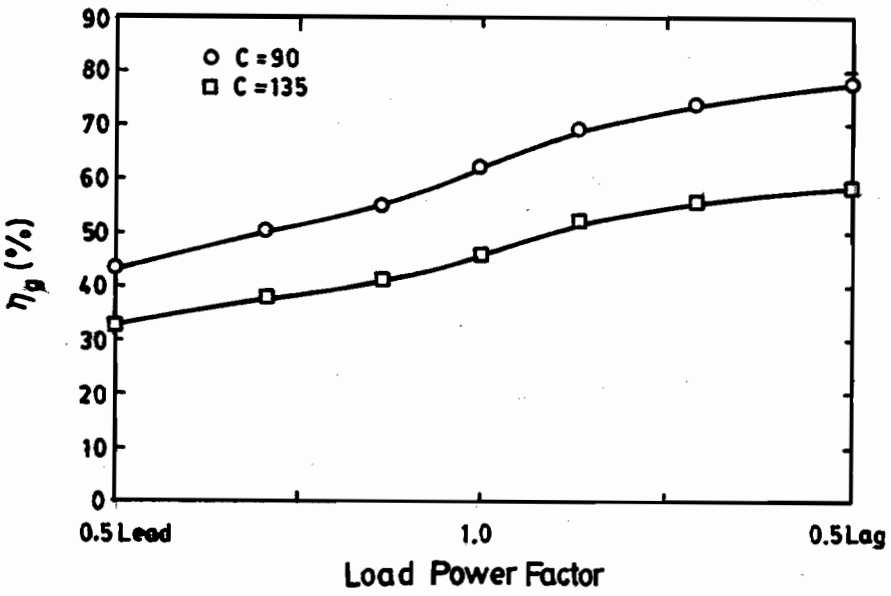

Fig. 14. Variation of efficiency with load power factor and C at rotor speed 1250 rpm.

as the drop in efficiency obtained for leading power factors, irrespective of the value of capacitance connected at the terminals of the generator.

CONCLUSIONS

The mathematical model reveals the importance of the magnetizing reactance and its role in the self-excitation process of an induction generator. The effective value of the magnetizing reactance varies in a nonlinear manner with respect to rotor speed, load impedance and load power factor. Such nonlinear behavior has two limiting values $X_{s\,\min}$ and $X_{s\,\max}$ within which the self-excitation process of an induction generator can be developed. Load power factor variations affect both the value of $X_{s\,\min}$ and the range of capacitance (i.e. $C_{\max} - C_{\min}$) necessary for the self-excitation process. The choice of the terminal capacitance and the load power factor will determine the value of both the output voltage and its frequency. The experimental results are in good agreement with the results obtained from the mathematical model, thereby proving the validity of the model.

ACKNOWLEDGEMENT

This work was supported by Research Grant No EE 053, Kuwait University.

REFERENCES

Grantham, C. 1985. Determination of induction motor parameter variations from a variable frequency standstill test. Electric Machines and Power Systems Journal **10**: 239–48.

Grantham, C., Sutanto, D. & Mismail, B. 1989. Steady-state and transient analysis of self-excited induction generators. Institute of Electrical Engineers Proceedings **136 B**: 61–68.

Malik, N.H. & Al-Bahrani, A.H. 1990. Influence of the terminal capacitor on the performance characteristics of a self-excited induction generator. Institute of Electrical Engineers Proceedings **137C**: 168–73.

Melkebeek, J.A.A. & Novotny, D.W. 1983a. Steady state modelling of regeneration and self-excitation in induction motor drives. Institute of Electrical and Electronic Engineering Transactions on Power Apparatus and Systems **102**: 2725–33.

Melkebeek, J.A.A. & Novotny, D.W. 1983b. The influence of saturation on induction machine drive dynamics. Institute of Electrical and Electronic Engineering Transactions on Industrial Applications **IA-19**: 671–81.

Murthy, S.S. & Tandon, A.K. 1985. New method of computing steady-state response of self-excited induction generator. Institute of Engineers (Indian) Journal **65**: 196–201.

Ouazene, L. & Macpherson, G. 1983. Analysis of the isolated induction generator. Institute of Electrical and Electronic Engineers Transactions on Power Apparatus and Systems **102**: 2793–98.

Salama, M.H. 1993. Design range of capacitance for self excitation of a stand-alone induction generator. Journal of the University of Kuwait (Science) **20 (1)**: 101–14.

Tandon, A.K., Murthy, S.S. & Berg, G.J. 1984. Steady-state analysis of capacitor self-excited induction generator. Institute of Electrical and Electronic Engineering Transactions on Power Apparatus and Systems **103**: 612–18.

Yegna Narayanan, S.S. & Johnny, V.J. 1986. Contributions to the steady-state analysis of wind-turbine driven self-excited induction generators. Institute of Electrical and Electronic Engineers Transactions on Energy Conversion **EC-1**: 169–76.

(Received 7 January 1992, revised 3 October 1992)

APPENDIX 1

THE EXPRESSIONS FOR R_L AND X_L

(a) For inductive load

$$R_L = \frac{RX_c^2}{aD}, \qquad X_L = \frac{X_c(XX_c + R^2 + a^2X^2)}{D}$$

(b) For pure resistive load

$$R_L = \frac{RX_c^2}{a(a^2R^2 + X_c^2)}, \qquad X_L = \frac{X_c R^2}{a^2R^2 + X_c^2}$$

(c) For capacitive load

$$R_L = \frac{RX_c^2}{aD}, \qquad X_L = \frac{X_c(-XX_2 + R^2 + a^2X^2)}{D}$$

(d) For no-load

$$R_L = 0 \qquad X_L = X_c/a^2$$

where $D = a^4X^2 + a^2(R^2 - 2XX_c) + X_c^2$

APPENDIX 2

THE COEFFICIENTS OF THE POLYNOMIAL

(1) For inductive load

$$P_0 = -bR_2(R^2X_c^2 + 2RR_1X_c^2 + R_1^2X_c^2)$$

$$P_1 = R_2(R^2X_c^2 + 2RR_1X_c^2 + R_1^2X_c^2) + (R_2^2 + b^2X_2^2)(RX_c^2 + R_1X_c^2)$$

$$P_2 = -bR_2(X_c^2X^2 + R_1^2R^2 - 2XX_cR_1^2 + X_1^2X_c^2 + 2X_1X_c^2X - 2X_1X_cR^2) - 2bX_2^2(RX_c^2 + R_1X_c^2)$$

$$P_3 = R_2(X_c^2X^2 + R_1^2R^2 - 2XX_cR_1^2 + X_1^2X_c^2 + 2X_1X_c^2X - 2X_1X_cR^2) + X_2^2(RX_c^2 + R_1X_c^2) + (R_2^2 + b^2X_2^2)(R_1R^2 - 2XX_cR_1)$$

$$P_4 = -bR_2(R_1^2X^2 + X_1^2R^2 - 2XX_cX_1^2 - 2X_1X_cX^2) - 2bX_2^2(R_1R^2 - 2XX_cR_1)$$

$$P_5 = R_2(R_1^2X^2 + X_1^2R^2 - 2XX_cX_1^2 - 2X_1X_cX^2) + X_2^2(R_1R^2 - 2XX_2R_1) + R_1X^2(R_2^2 + b^2X_2^2)$$

$$P_6 = -bR_2X_1^2X^2 - 2bX_2^2R_1X^2$$

$$P_7 = X_2^2R_1X + R_2X_1^2X^2$$

(2) For pure resistive load

The coefficients of the polynomial can be obtained from case (1) by substituting $X = 0$.

(3) For the no-load condition

$$P_0 = -bR_2X_c^2$$

$$P_1 = R_2X_c^2$$

$$P_2 = 2bR_2X_1X_c - bR_2R_1^2$$

$$P_3 = -2X_1X_cR_2 + R_2^2R_1 + b^2X_2^2R_1 + R_2R_1^2$$

$$P_4 = -2bX_2^2R_1 - bR_2X_1^2$$

$$P_5 = X_2^2R_1 + R_2X_1^2$$

$$P_6 = 0$$

$$P_7 = 0$$

(4) For capacitive load

$$P_0 = -bR_2(R^2X_c^2 + 2R_1RX_c^2 + R_1^2X_c^2)$$

$$P_1 = R_2(R^2X_c^2 + 2R_1RX_c^2 + R_1^2X_c^2) + (R_2^2 + bX_2^2)(R_1X_c^2 + RX_c^2)$$

$$P_2 = -bR_2(X_c^2X^2 + R_1^2R^2 + 2XX_cR_1^2 - 2X_1X_c^2X - 2X_1X_cR^2 + X_1^2X_c^2) - 2bX_2^2(R_1X_c^2 + RX_c^2)$$

$$P_3 = R_2(X_c^2X^2 + R_1^2R^2 + 2XX_cR_1^2 - 2X_1X_c^2X - 2X_1X_cR^2 + X_1^2X_c^2) + X_2^2(R_1X_c^2 + RX_c^2) + (R_2^2 + b^2X_2^2)(R_1R^2 + 2XX_cR_1)$$

$$P_4 = -bR_2(R_1^2X^2 - 2X_1X_cX^2 + X_1^2R^2 + 2XX_cX_1^2) - 2bX_2^2(R_1R^2 + 2XX_cR_1)$$

$$P_5 = R_2(R_1^2X^2 - 2X_1X_cX^2 + X_1^2R^2 + 2XX_cX_1^2) + X_2^2(R_1R^2 + 2XX_cR_1) + (R_2^2 + b^2X_2^2)(R_1X^2)$$

$$P_6 = -bR_2(X_1^2X^2) - 2bX_2^2(R_1X^2)$$

$$P_7 = X_2^2(R_1X^2) + R_2(X_1^2X^2)$$

دور الممانعة المغناطيسية في أداء حالة الاستقرار للمولدات التأثيرية

محمد حسن سلامه
قسم الهندسة الكهربائية والكمبيوتر بجامعة الكويت
ص.ب. ٥٩٦٩، الصفاة ١٣٠٦٠، الكويت

خلاصة

يقدم البحث طريقة حسابية للحصول على خواص التحميل لمولد تأثيري. وتعتمد الطريقة الحسابية على نموذج رياضي مشتق من الدائرة الكهربائية المكافئة لمولد تأثيري في حالة الاستقرار. في هذا النموذج الرياضي تعتبر القيمة الصغرى لسعة المكثف اللازم لبدء عملية إثارة المولد هي العنصر المؤثر فيه. وتعتمد القيمة الصغرى لسعة المكثف على كل من نوعية وقيمة الحمل بالإضافة إلى سرعة دوران المولد.

من المعلوم أن الممانعة المغناطيسية للمولد التأثيري تكون لاخطية كما أنها تتأثر بقيمة سعة المكثف المستعمل بغرض إثارة المولد. ولقد أدت هذه العلاقة بين الممانعة المغناطيسية وقيمة سعة المكثف إلى نتيجة هامة توضح أن هناك قيمة صغرى وقيمة عظمى للممانعة المغناطيسية.

في هذا البحث تم حساب قيمة كل من الجهد الخارج والتردد المناظر له وكفاءة المولد التأثيري وذلك عند أحمال مختلفة ذات معاملات قدرة متغيرة. وعند مقارنة بعض هذه النتائج النظرية بنظيراتها التي أمكن الحصول عليها من التجارب العملية، لوحظ تقارب شديد بينهما مما يعطي الثقة في مستوى النموذج الرياضي الذي يمثل أداء حالة الاستقرار للمولد التأثيري.

ويمثل هذا النموذج، بعد التأكد من تطابقه مع الأداء الفعلي للمولد التأثيري، وسيلة بسيطة ومباشرة لدراسة تعويض القدرة غير الفعالة عند تعميم دوائر المولدات التأثيرية.